Original Article | Gastrointestinal Imaging

eISSN 2005-8330
https://doi.org/10.3348/kjr.2019.0406
Korean J Radiol 2020;21(1):77-87

Korean Journal of Radiology
KJR

Check for updates

Feasibility of Simultaneous Multislice Acceleration Technique in Diffusion-Weighted Magnetic Resonance Imaging of the Rectum

Jae Hyon Park, MD[1], Nieun Seo, MD, PhD[1], Joon Seok Lim, MD, PhD[1], Jongmoon Hahm, BS[2], Myeong-Jin Kim, MD, PhD[1]

[1]Department of Radiology, Severance Hospital, Yonsei University College of Medicine, Seoul, Korea; [2]Siemens Healthineers Korea, Seoul, Korea

Objective: To assess the feasibility of simultaneous multislice-accelerated diffusion-weighted imaging (SMS-DWI) of the rectum in comparison with conventional DWI (C-DWI) in rectal cancer patients.

Materials and Methods: This study included 65 patients with initially-diagnosed rectal cancer. All patients underwent C-DWI and SMS-DWI with acceleration factors of 2 and 3 (SMS2-DWI and SMS3-DWI, respectively) using a 3T scanner. Acquisition times of the three DWI sequences were measured. Image quality in the three DWI sequences was reviewed by two independent radiologists using a 4-point Likert scale and subsequently compared using the Friedman test. Apparent diffusion coefficient (ADC) values for rectal cancer and the normal rectal wall were compared among the three sequences using repeated measures analysis of variance.

Results: Acquisition times using C-DWI, SMS2-DWI, and SMS3-DWI were 173 seconds, 107 seconds, (38.2% shorter than C-DWI), and 77 seconds (55.5% shorter than C-DWI), respectively. For all image quality parameters other than distortion (margin sharpness, artifact, lesion conspicuity, and overall image quality), C-DWI and SMS2-DWI yielded better results than did SMS3-DWI (Ps < 0.001), with no significant differences observed between C-DWI and SMS2-DWI (Ps ≥ 0.054). ADC values of rectal cancer (p = 0.943) and normal rectal wall (p = 0.360) were not significantly different among C-DWI, SMS2-DWI, and SMS3-DWI.

Conclusion: SMS-DWI using an acceleration factor of 2 is feasible for rectal MRI resulting in substantial reductions in acquisition time while maintaining diagnostic image quality and similar ADC values to those of C-DWI.

Keywords: *Diffusion-weighted imaging; Rectum; Rectal cancer; Simultaneous multislice*

INTRODUCTION

Colorectal cancer is a common malignancy, and rectal cancer accounts for approximately one-third of colorectal cancer cases (1). In rectal cancer patients, magnetic resonance imaging (MRI) is the primary imaging modality, principally due to its exceptionally excellent soft tissue contrast in T2-weighted imaging (2, 3). In addition to T2-weighted imaging, diffusion-weighted imaging (DWI), a functional MRI technique, helps not only in detecting and characterizing lesions, but also in predicting the therapeutic response in rectal cancer (4-8). Furthermore, because DWI does not require intravenous contrast administration, it is generally implemented as part of a routine MRI protocol in evaluation of rectal cancer (9).

However, the use of DWI is limited by its relatively long scan time, which can cause motion artifacts due to bowel peristalsis, and patient discomfort. Techniques aimed at decreasing DWI scan time have thus emerged as a topic of great interest. Recently, the simultaneous multislice (SMS) technique was reported as a novel means of making DWI faster (10-12). This technique involves simultaneous excitation and acquisition of multiple slices, enabling a reduction in scan time based on a greater number

Received June 12, 2019; accepted after revision September 17, 2019.

Corresponding author: Nieun Seo, MD, PhD, Department of Radiology, Severance Hospital, Yonsei University College of Medicine, 50-1 Yonsei-ro, Seodaemun-gu, Seoul 03722, Korea.
• Tel: (822) 2228-7400 • Fax: (822) 2227-8337
• E-mail: sldmsdl@yuhs.ac

This is an Open Access article distributed under the terms of the Creative Commons Attribution Non-Commercial License (https://creativecommons.org/licenses/by-nc/4.0) which permits unrestricted non-commercial use, distribution, and reproduction in any medium, provided the original work is properly cited.

Copyright © 2020 The Korean Society of Radiology

of simultaneously excited slices as determined by the acceleration factor. Linear combinations of signals from each of the slices, weighted by the spatial coil sensitivity profiles, are then received by a radiofrequency coil channel, and matrix inversion is used to reconstruct the signal for each individual slice. In this technique, the number of slices acquired over the same pulse repetition time can be increased by setting a higher acceleration factor without the need for an increase in the gradient demand (10-12).

Several recent studies have reported the successful application of the SMS technique in DWI and diffusion tensor imaging of the brain, skeletal and cardiac muscles, liver, pancreas, kidney, pelvic lymph nodes, and prostate (13-19). However, the SMS technique has not yet been applied in DWI of the rectum. Unlike other organs, the image quality of rectal DWI can be affected by motion artifacts, distortion, and susceptibility artifacts by the rectum and adjacent bowel loops. Although the use of spasmolytics is useful in reducing bowel movement artifacts in rectal MRI, patients with contraindications to spasmolytics such as scopolamine butylbromide, including those with narrow angle glaucoma or obstructive prostate hypertrophy, have limited use of spasmolytics (20). In these patients, a short scan time is particularly important to avoid image degradation during DWI. In addition, lesion detection capabilities and apparent diffusion coefficient (ADC) values should be validated for rectal cancer so that the SMS technique can be incorporated into routine clinical applications.

Therefore, we aimed to investigate the feasibility of DWI of the rectum by using the SMS technique (SMS-accelerated DWI, SMS-DWI) in patients with rectal cancer and to compare the image quality of SMS-DWI sequences with different acceleration factors to the conventional DWI (C-DWI) sequence.

MATERIALS AND METHODS

Patients

This study was approved by our Institutional Review Board, and the requirement for written informed consent was waived due to the retrospective study design. We analyzed DWI data acquired during clinical adaption of our institutional rectal MRI protocol using a 3T scanner. Patients who had undergone rectal MRI with this machine between February 2018 and July 2018 were consecutively recruited. Among the 202 patients who had undergone rectal MRI, 137 were excluded on the basis of the following criteria: 1) no pathologically confirmed rectal adenocarcinoma (n = 36), 2) rectal MRI after preoperative chemoradiotherapy for rectal cancer (n = 82), and 3) postoperative rectal MRI (n = 19). Finally, 65 patients (male, 34; female, 31; mean age ± standard deviation, 63.1 ± 12.0 years) who had undergone rectal MRI due to initially diagnosed rectal cancer were included in this study (Fig. 1). Histological differentiation of rectal cancer was as follows: well-differentiated adenocarcinoma in seven patients (10.7%), moderately differentiated adenocarcinoma in 56 patients (86.2%), and poorly differentiated adenocarcinoma in two patients (3.1%).

MRI Acquisition

Rectal MRI was performed using a 3T scanner (MAGNETOM Prisma^{Fit}, Siemens Healthineers, Erlangen, Germany) with a 30-channel anterior surface body coil and a 32-channel spine coil (which actually used 24 and 12 channels, respectively, for axial slice coverage). Approximately 5 minutes before MRI scanning, 20 mg of scopolamine

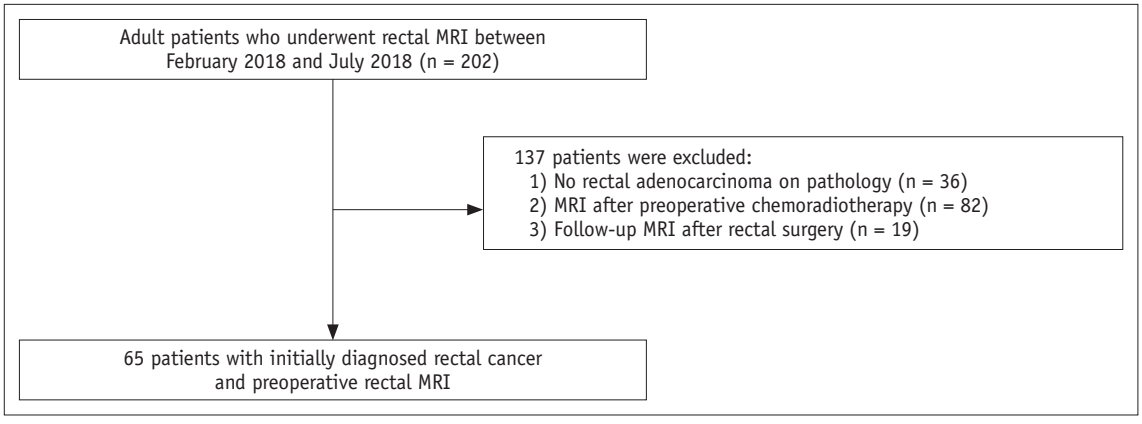

Fig. 1. Flow diagram of study population.

https://doi.org/10.3348/kjr.2019.0406

Korean Journal of Radiology
KJR

butylbromide was injected intramuscularly to reduce bowel peristalsis, unless it was contraindicated. If the lesion was assumed to be in the middle or lower rectum, endorectal filling with approximately 50–100 mL of sonographic transmission gel was performed; thus, the gel was used in all except seven patients (five patients with upper rectal tumors, one patient with a previous history of anal fistulectomy, and one patient who refused the procedure). T2-weighted images were obtained in the axial, sagittal, oblique axial, and coronal orientations using a respiratory-triggered echo train spin echo sequence. In all patients, three echo-planar imaging-based DWI sequences were acquired in the following order: C-DWI and SMS-DWI with acceleration factors of 2 (SMS2-DWI) and 3 (SMS3-DWI). All DWI sequences were acquired via a monopolar diffusion sensitizing gradient applied in three orthogonal directions with b-values of 0, 300, and 1000 s/mm^2. For DWI sequences, spectral attenuated inversion recovery fat saturation was applied along with standard automatic shimming. The detailed acquisition parameters are summarized in Table 1.

Qualitative Image Analysis

Two board-certified abdominal radiologists with 6 years and 17 years of experience in rectal MRI, respectively, independently reviewed the DWI images. They were aware that all patients had undergone rectal MRI due to initially diagnosed rectal cancer. Prior to the image review, another radiologist (one junior radiology resident) anonymized the three sets of DWI data (C-DWI, SMS2-DWI, and SMS3-DWI) to conceal information on patient demographics, identification numbers, and specific DWI sequences. Then, he randomly assigned a number to each DWI set. Three image sets and T2-weighted images were simultaneously provided to both radiologists who were completely blinded to the DWI sequences and other clinical information such as the location of rectal cancer.

Before evaluation of DWI sequences, the tumor was identified using T2-weighted images. Subjective parameters of image quality (i.e., margin sharpness, distortion, artifacts, lesion conspicuity, and overall image quality) were evaluated based on a 4-point Likert scale, with higher scores indicating better image quality. Margin sharpness, distortion, artifacts, and lesion conspicuity were assessed in DWI images (b = 1000 s/mm^2), whereas overall image quality was evaluated in both DWI images (b = 1000 s/mm^2) and ADC maps. For margin sharpness, the following scores indicated the respective sharpness levels of normal anatomic structures: 1, not sharp; 2, slightly sharp; 3, moderately sharp; and 4, very sharp. For distortion, the following scores indicated the respective distortion levels: 1, presence of severe distortion; 2, moderate distortion; 3, mild distortion; and 4, no distortion. For ghosting, motion, and susceptibility artifacts, a score of 1 was assigned if there were severe artifacts causing diagnostic difficulty, 2 for moderate artifacts, 3 for mild artifacts, and 4 for no artifacts. Lesion conspicuity

Table 1. Scan Parameters for DWI Sequences

Scan Parameters	C-DWI	SMS2-DWI	SMS3-DWI
Repetition time, ms	6700	3700	2500
Echo time, ms	63	72	74
Slice thickness, mm	5	5	5
Number of slices	40	40	40
Bandwidth, Hz/px	1860	1860	1860
Echo spacing, ms	0.6	0.6	0.6
Voxel size, mm^3	1.7 x 1.7 x 5	1.7 x 1.7 x 5	1.7 x 1.7 x 5
iPAT	GRAPPA 2	GRAPPA 2	GRAPPA 2
SMS AF	-	2	3
Fat saturation	SPAIR	SPAIR	SPAIR
Diffusion mode	4-scan trace	4-scan trace	4-scan trace
Concatenations	1	1	1
b-values, s/mm^2 (averages)	0 (2), 300 (2), 1000 (3)	0 (2), 300 (2), 1000 (3)	0 (2), 300 (2), 1000 (3)
Scan time, sec	173	107	77

C-DWI = conventional DWI, DWI = diffusion-weighted imaging, GRAPPA = generalized autocalibrating partially parallel acquisition, iPAT = integrated parallel acquisition technique, SMS = simultaneous multislice, SMS AF = SMS acceleration factor, SMS2-DWI = SMS accelerated DWI with acceleration factor of 2, SMS3-DWI = SMS accelerated DWI with acceleration factor of 3, SPAIR = spectral attenuated inversion recovery

https://doi.org/10.3348/kjr.2019.0406

was assessed as 1 if the rectal cancer lesion was difficult to detect, 2 if it was minimally recognizable, 3 if it was moderately conspicuous, and 4 if it was very conspicuous. Overall image quality was graded as follows: 1, poor; 2, fair; 3, good; and 4, excellent.

Quantitative Image Analysis

All digital imaging and communication in medicine data from DWI were transferred to a commercial three-dimensional software program (Aquarius iNtuition version 4.4.12, TeraRecon Inc., Foster City, CA, USA). For quantitative analysis, the junior radiology resident and a board-certified abdominal radiologist performed region of interest (ROI) measurements in consensus. Two ROIs were drawn on consecutive ADC images to include the largest areas of rectal cancer and normal rectal wall, respectively. Averages of the two ROI measurements were then used for statistical analysis. ROIs were placed at the same respective locations on ADC maps as in C-DWI, SMS2-DWI, and SMS3-DWI using the software's ROI copy-and-paste function. Mean areas of the ROIs were 65.3 ± 128.3 mm^2 for rectal cancer and 13.1 ± 8.2 mm^2 for the normal rectal wall.

Statistical Analysis

Image quality scores and ADC values were expressed as means and standard deviations. The averages of the values obtained by the two readers were used for the following statistical analyses, and the original data were used to calculate interobserver agreement. Normal distribution of the data was tested using the Kolmogorov-Smirnov test. Qualitative image parameters were compared among the three DWI sequences (C-DWI, SMS2-DWI, and SMS3-DWI) using the Friedman test. In cases where the Friedman test showed statistical significance, the Dunn-Bonferroni post-hoc test was performed to analyze all pairwise comparisons. Interobserver agreement of image quality was analyzed using weighted κ statistics as follows: κ values < 0.20, poor agreement; 0.21–0.40, fair; 0.41–0.60, moderate; 0.61–0.80, good; and 0.81–1.00, excellent. ADC values among the C-DWI, SMS2-DWI, and SMS3-DWI sequences were compared using one-way repeated measures analysis of variance. In addition, ADC values for rectal cancer and the normal rectal wall for each DWI sequence were compared using paired *t* test. For qualitative and quantitative analyses, subgroup analyses were performed according to the location of the rectal cancer (upper, middle, lower) and usage of endorectal gel. Statistical analyses were performed using the SPSS v23.0 software (IBM Corp., Armonk, NY, USA) and MedCalc Statistical Software version 18.2.1 (MedCalc Software bvba, Mariakerke, Belgium). $P < 0.05$ was considered statistically significant.

RESULTS

SMS2-DWI and SMS3-DWI of the rectum were successfully performed in all patients. Tumors were located in the upper (n = 13), middle (n = 33), and lower (n = 19) rectum. Acquisition times were 173 seconds, 107 seconds, and 77 seconds for C-DWI, SMS2-DWI, and SMS3-DWI, respectively. The acquisition times of SMS2-DWI (107 seconds) and SMS3-DWI (77 seconds) were 38.2% and 55.5% shorter than that of C-DWI (173 seconds). Representative DWI and ADC maps of C-DWI, SMS2-DWI, and SMS3-DWI are shown in Figures 2 and 3.

Qualitative Analysis

A detailed summary of image quality scores for the three DWI sequences in all patients is provided in Table 2. The degree of image distortion was not significantly different among C-DWI (2.76 ± 0.51), SMS2-DWI (2.78 ± 0.48), and SMS3-DWI (2.78 ± 0.48; $p = 0.526$). In contrast, margin sharpness, artifacts, lesion conspicuity, and overall image quality were significantly different among the three DWI sequences (Ps < 0.001). For all image quality ratings except distortion, C-DWI and SMS2-DWI exhibited better image quality than SMS3-DWI ($p < 0.001$), with no significant differences observed between C-DWI and SMS2-DWI ($p \geq 0.054$). The mean score of overall image quality of SMS2-DWI (b = 1000 s/mm^2) was slightly higher (3.65 ± 0.36) than that of C-DWI (3.50 ± 0.44), without a significant difference ($p = 0.054$).

Subgroup analysis according to tumor location showed similar trends for margin sharpness, distortion, and artifacts (Table 3) in comparison with the analysis in all patients. However, for lesion conspicuity, there was no significant difference between C-DWI and SMS3-DWI in middle and lower rectal cancer ($p = 0.348$ and $p = 0.057$, respectively). For overall image quality, there was no significant difference between C-DWI and SMS3-DWI in middle rectal cancer on b1000 images ($p = 0.051$) and upper rectal cancer on ADC maps ($p = 0.051$). In patients who received gel distension (n = 58), subgroup analysis of image quality scores showed similar results as those obtained for all cases (Table 3). In those without gel distension, the differences between SMS2-DWI and SMS3-DWI and between C-DWI and SMS3-

https://doi.org/10.3348/kjr.2019.0406

Korean Journal of Radiology
KJR

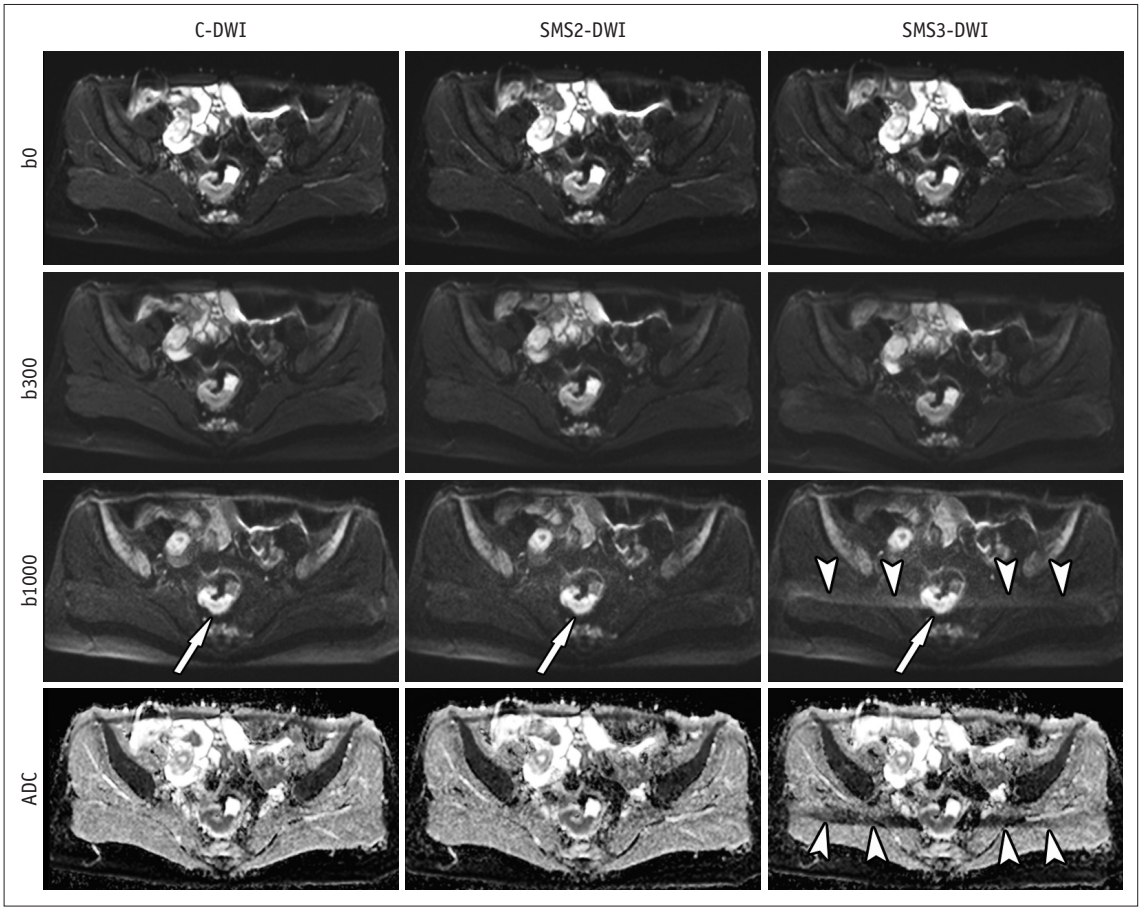

Fig. 2. C-DWI and SMS2-DWI and SMS3-DWI in 41-year-old female with rectal cancer. Image set consists of b0, b300, b1000, and ADC map. Image quality and lesion conspicuity for rectal cancer (arrows) in SMS2-DWI (overall image quality score: 4 by both readers) are not significantly different from those in C-DWI (score: 4 by both readers). However, SMS3-DWI (score: 3 in both readers) shows significant aliasing artifacts (arrowheads) and worse image quality in comparison with C-DWI and SMS2-DWI. b0, b = 0 s/mm^2; b300, b = 300 s/mm^2; b1000, b = 1000 s/mm^2. ADC = apparent diffusion coefficient, C-DWI = conventional DWI, DWI = diffusion-weighted imaging, SMS = simultaneous multislice, SMS2-DWI = SMS accelerated DWI with acceleration factor of 2, SMS3-DWI = SMS accelerated DWI with acceleration factor of 3

DWI were not significant for sharpness, artifacts, lesion conspicuity, and overall image quality.

Interobserver agreement for image quality assessment was good, with a κ value of 0.71 (95% confidence interval [CI], 0.54–0.88) for C-DWI, 0.73 (95% CI, 0.52–0.94) for SMS2-DWI, and 0.65 (95% CI, 0.34–0.97) for SMS3-DWI.

Quantitative Analysis

The ADC values measured in rectal cancer and the normal rectal wall in C-DWI, SMS2-DWI, and SMS3-DWI are summarized in Table 4. ADC values were not significantly different among the three DWI sequences for rectal cancer (p = 0.943) and normal rectal wall (p = 0.360). Subgroup analysis according to the location of rectal cancer and gel usage showed similar results. The results from Bland-Altman plots are demonstrated in Figure 4. In all three sequences, mean ADC values were significantly lower in rectal cancer in comparison with those for the normal rectal wall (p < 0.001 for all three sequences).

DISCUSSION

Our study demonstrated that SMS-DWI of the rectum was feasible in patients with rectal cancer. Furthermore, there was a considerable reduction in acquisition time with the SMS technique. With SMS2-DWI, acquisition time was reduced by approximately 40% of that of C-DWI while preserving overall image quality and lesion conspicuity. With SMS3-DWI, although acquisition time was reduced by approximately 60% of that of C-DWI, image quality deteriorated significantly. In addition, quantitatively measured ADC values of rectal cancer and normal rectal wall were not significantly different among C-DWI, SMS2-DWI, and SMS3-DWI. Overall, our study revealed that SMS2-DWI

https://doi.org/10.3348/kjr.2019.0406

of the rectum is an acceptable method for DWI acquisition that is faster than C-DWI and shows no significant compromise in image quality.

Our study also found that acceleration factors ≥ 3 in SMS-DWI of the rectum significantly decreased all image quality ratings except for distortion. Indeed, MR images obtained with SMS3-DWI showed profound ghosting artifacts, resulting in decreased image quality for both high b-value DWI (b = 1000 s/mm^2) and ADC maps. The lesion conspicuity for rectal cancer was worse in SMS3-DWI than in

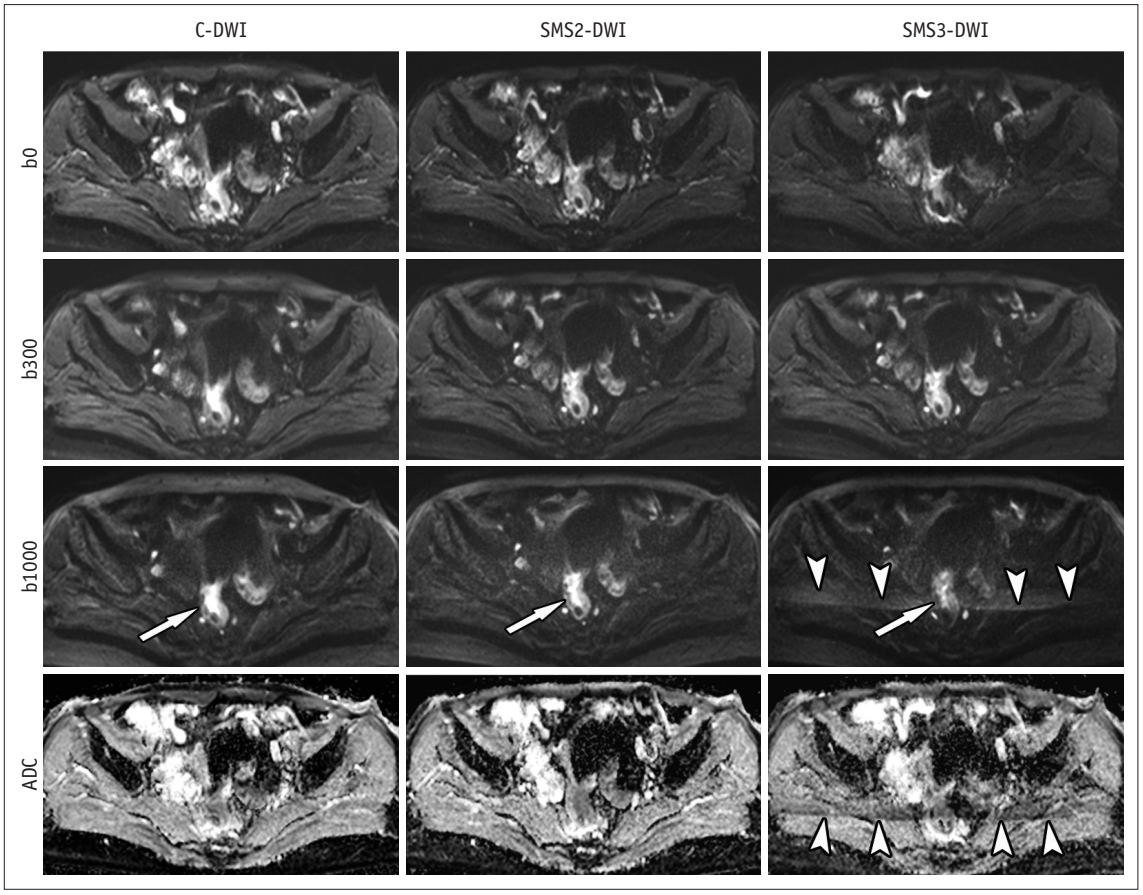

Fig. 3. C-DWI and SMS2-DWI and SMS3-DWI in 66-year-old female with rectal cancer. Image set consists of b0, b300, b1000, and ADC map. Image quality and lesion conspicuity for rectal cancer (arrows) in SMS2-DWI are not significantly different from those in C-DWI. However, SMS3-DWI shows decreased lesion conspicuity (arrow) and significant aliasing artifacts (arrowheads) in comparison with C-DWI and SMS2-DWI. Overall image quality scores were 3, 4, and 2 for C-DWI, SMS2-DWI, and SMS3-DWI by both readers. b0, b = 0 s/mm^2; b300, b = 300 s/mm^2; b1000, b = 1000 s/mm^2.

Table 2. Image Quality Scores

Parameters	C-DWI	SMS2-DWI	SMS3-DWI	*P**	*P*†: C vs. SMS2	*P*†: SMS2 vs. SMS3	*P*†: C vs. SMS3
Sharpness	3.54 ± 0.47	3.58 ± 0.40	3.02 ± 0.50	< 0.001	> 0.999	< 0.001	< 0.001
Distortion	2.76 ± 0.51	2.78 ± 0.48	2.78 ± 0.48	0.526			
Artifact	3.48 ± 0.40	3.42 ± 0.37	2.84 ± 0.38	< 0.001	0.441	< 0.001	< 0.001
Lesion conspicuity	3.67 ± 0.52	3.67 ± 0.54	3.42 ± 0.36	< 0.001	> 0.999	< 0.001	< 0.001
Overall image quality							
b1000	3.50 ± 0.44	3.65 ± 0.36	3.06 ± 0.46	< 0.001	0.054	< 0.001	< 0.001
ADC	3.49 ± 0.45	3.50 ± 0.39	3.13 ± 0.40	< 0.001	> 0.999	< 0.001	< 0.001

Means and standard deviations of image quality obtained by two radiologists are summarized. Sharpness, artifact, and lesion conspicuity were evaluated in DWI (b1000). *p values were obtained from overall comparison among C-DWI, SMS2-DWI, and SMS3-DWI, †Dunn-Bonferroni post-hoc test was performed in case of significant differences in overall Friedman test. b1000, b = 1000 s/mm^2. ADC = apparent diffusion coefficient

https://doi.org/10.3348/kjr.2019.0406

Korean Journal of Radiology
KJR

Table 3. Subgroup Analysis of Image Quality Scores according to Tumor Location and Usage of Endorectal Gel

Parameters	C-DWI	SMS2-DWI	SMS3-DWI	*P**	*P*†: C vs. SMS2	*P*†: SMS2 vs. SMS3	*P*†: C vs. SMS3
Sharpness (n = 65)							
Tumor location							
Upper (n = 13)	3.62 ± 0.30	3.46 ± 0.32	3.04 ± 0.48	0.002	0.306	0.054	0.021
Middle (n = 33)	3.55 ± 0.52	3.65 ± 0.40	3.09 ± 0.52	< 0.001	0.990	< 0.001	0.003
Lower (n = 19)	3.50 ± 0.47	3.53 ± 0.42	2.89 ± 0.49	< 0.001	> 0.999	< 0.001	0.003
Gel distension							
Gel (n = 58)	3.55 ± 0.48	3.59 ± 0.39	3.03 ± 0.50	< 0.001	> 0.999	< 0.001	< 0.001
No gel (n = 7)	3.50 ± 0.47	3.50 ± 0.50	3.00 ± 0.58	0.040	> 0.999	0.114	0.198
Distortion							
Tumor location							
Upper	2.96 ± 0.52	2.96 ± 0.52	3.00 ± 0.46	0.717	-	-	-
Middle	2.73 ± 0.47	2.76 ± 0.45	2.74 ± 0.45	0.549	-	-	-
Lower	2.66 ± 0.55	2.68 ± 0.51	2.68 ± 0.51	0.846	-	-	-
Gel distension							
Gel	2.77 ± 0.45	2.78 ± 0.42	2.78 ± 0.41	0.735	-	-	-
No gel	2.64 ± 0.90	2.71 ± 0.91	2.71 ± 0.91	0.368	-	-	-
Artifact							
Tumor location							
Upper	3.58 ± 0.34	3.54 ± 0.38	3.00 ± 0.35	0.001	> 0.999	0.018	0.033
Middle	3.41 ± 0.42	3.35 ± 0.34	2.80 ± 0.35	< 0.001	0.753	< 0.001	< 0.001
Lower	3.53 ± 0.39	3.47 ± 0.39	2.79 ± 0.42	< 0.001	> 0.999	< 0.001	< 0.001
Gel distension							
Gel	3.47 ± 0.41	3.41 ± 0.38	2.82 ± 0.36	< 0.001	0.411	< 0.001	< 0.001
No gel	3.50 ± 0.29	3.50 ± 0.29	3.00 ± 0.50	0.008	> 0.999	0.060	0.114
Lesion conspicuity							
Tumor location							
Upper	3.81 ± 0.33	3.81 ± 0.33	3.35 ± 0.43	< 0.001	> 0.999	0.006	0.006
Middle	3.81 ± 0.33	3.62 ± 0.57	3.48 ± 0.63	0.032	> 0.999	0.039	0.348
Lower	3.63 ± 0.60	3.66 ± 0.60	3.37 ± 0.68	0.003	> 0.999	0.024	0.057
Gel distension							
Gel	3.67 ± 0.51	3.69 ± 0.52	3.47 ± 0.60	< 0.001	> 0.999	< 0.001	0.003
No gel	3.57 ± 0.61	3.50 ± 0.71	3.07 ± 0.61	0.015	0.951	0.177	0.306
Overall image quality							
b1000							
Tumor location							
Upper	3.62 ± 0.36	3.65 ± 0.38	2.96 ± 0.43	< 0.001	> 0.999	0.009	0.021
Middle	3.41 ± 0.49	3.64 ± 0.36	3.14 ± 0.46	< 0.001	0.087	< 0.001	0.051
Lower	3.58 ± 0.38	3.66 ± 0.37	3.00 ± 0.47	< 0.001	0.150	< 0.001	0.003
Gel distension							
Gel	3.53 ± 0.44	3.66 ± 0.36	3.08 ± 0.45	< 0.001	0.111	< 0.001	< 0.001
No gel	3.29 ± 0.39	3.50 ± 0.41	2.93 ± 0.53	0.031	0.771	0.069	0.471
ADC							
Tumor location							
Upper	3.54 ± 0.38	3.58 ± 0.40	3.08 ± 0.53	0.003	> 0.999	0.015	0.051
Middle	3.44 ± 0.53	3.48 ± 0.38	3.15 ± 0.38	< 0.001	> 0.999	0.003	0.018
Lower	3.53 ± 0.35	3.47 ± 0.39	3.13 ± 0.33	0.001	> 0.999	0.006	0.006
Gel distension							
Gel	3.50 ± 0.46	3.49 ± 0.38	3.14 ± 0.37	< 0.001	> 0.999	< 0.001	< 0.001
No gel	3.36 ± 0.38	3.57 ± 0.45	3.07 ± 0.61	0.104			

Mean values and standard deviation of image quality obtained by two radiologists are summarized. Sharpness, artifact, lesion conspicuity were evaluated on DWI (b1000). **p* values are obtained from overall comparison among C-DWI, SMS2-DWI, and SMS3-DWI, †Dunn-Bonferroni post-hoc test was performed in case of significant difference in overall Friedman test. b1000, b = 1000 s/mm^2.

https://doi.org/10.3348/kjr.2019.0406

Table 4. ADC Values

	C-DWI	SMS2-DWI	SMS3-DWI	*P*
Rectal cancer (n = 65)	0.84 ± 0.12	0.84 ± 0.13	0.84 ± 0.12	0.943
Tumor location				
Upper (n = 13)	0.88 ± 0.89	0.88 ± 0.12	0.88 ± 0.84	0.735
Middle (n = 33)	0.83 ± 0.11	0.82 ± 0.12	0.83 ± 0.12	0.148
Lower (n = 19)	0.84 ± 0.14	0.85 ± 0.15	0.84 ± 0.14	0.142
Gel distension				
Gel (n = 58)	0.83 ± 0.16	0.83 ± 0.16	0.83 ± 0.16	0.780
No gel (n = 7)	0.89 ± 0.93	0.83 ± 0.97	0.87 ± 0.73	0.102
Normal rectal wall	1.54 ± 0.15	1.55 ± 0.15	1.55 ± 0.15	0.360
Tumor location				
Upper	1.49 ± 0.14	1.50 ± 0.12	1.50 ± 0.13	0.794
Middle	1.57 ± 0.15	1.58 ± 0.13	1.57 ± 0.15	0.743
Lower	1.52 ± 0.16	1.53 ± 0.17	1.53 ± 0.17	0.340
Gel distension				
Gel	1.54 ± 0.19	1.55 ± 0.19	1.55 ± 0.20	0.379
No gel	1.50 ± 0.20	1.51 ± 0.17	1.52 ± 0.19	0.459

Mean ADC values (x 10^{-3} mm^2/s) and standard deviations are presented. *p* values are obtained from comparison of ADC values among C-DWI, SMS2-DWI, and SMS3-DWI using one-way repeated measure analysis of variance.

SMS2-DWI and C-DWI, which may indicate worse diagnostic ability of SMS3-DWI. These findings correspond with the results of previous studies in other organs (15, 16, 21). The poor image quality in SMS-DWI with a high acceleration factor can be explained by the increasing geometry factor, which is related to image heterogeneity and signal-to-noise ratio (SNR) reduction (22, 23). Therefore, routine clinical application of SMS-DWI with higher acceleration factors (≥ 3) would not be feasible in rectal MRI despite the significant scan time reduction.

The ADC values in rectal cancer and normal rectal wall measured in the present study were not significantly different among C-DWI, SMS2-DWI, and SMS3-DWI. A few previous studies have reported decreased ADC values using SMS-DWI in the liver and pancreas in comparison with C-DWI (14, 21, 24, 25). These studies hypothesized that the elevated noise floor in SMS-DWI may result in generally lower ADC values (21). However, several subsequent studies reported no significant differences in ADC values between SMS-accelerated sequences and C-DWI in several organs (15, 16, 26), which is in line with our results. Given that the ADC values of rectal cancer may reflect cancer aggressiveness by predicting the histologic T stage and differentiation (4, 27, 28) and that quantitative ADC measurement is useful in evaluating therapeutic response in rectal cancer after chemoradiotherapy (6-8), the comparable ADC values obtained with C-DWI and SMS-DWI in our study might be a prerequisite for reliable measurements and interpretation of ADC.

This study has several limitations. First, an inherent selection bias may exist due to the retrospective study design. Because we only included patients initially diagnosed with rectal cancer, patients who underwent rectal DWI for diseases other than rectal cancer or for evaluation of therapeutic response in rectal cancer should be evaluated in further studies to generalize our study results. Second, the relatively small sample size may limit the statistical power of subgroup analysis, particularly in those without gel distension. However, to the best of our knowledge, this is the first report investigating the feasibility of SMS-DWI in rectal cancer patients. Nonetheless, further large-scale studies may be required to validate our results. Third, because the three DWI sequences were obtained in the same order of C-DWI, SMS2-DWI, and SMS3-DWI for all patients, the time-dependent decrease in the efficacy of the antispasmolytic could have contributed to the worse image quality of SMS3-DWI. Nevertheless, the overall image quality of SMS2-DWI was comparable to that of C-DWI. Fourth, the acquisition times of DWI sequences were estimated times in this study. Fifth, we did not compare the SNR obtained with the three DWI sequences. For parallel imaging or an SMS-accelerated technique, a subtraction method using two stacks of images with identical scanning is recommended for SNR measurement (15, 19, 29). However, we could not obtain two image sets of the same sequences in routine clinical practice. Lastly, this study was conducted using only one type of scanner, the 3T MR scanner; a comparison

https://doi.org/10.3348/kjr.2019.0406

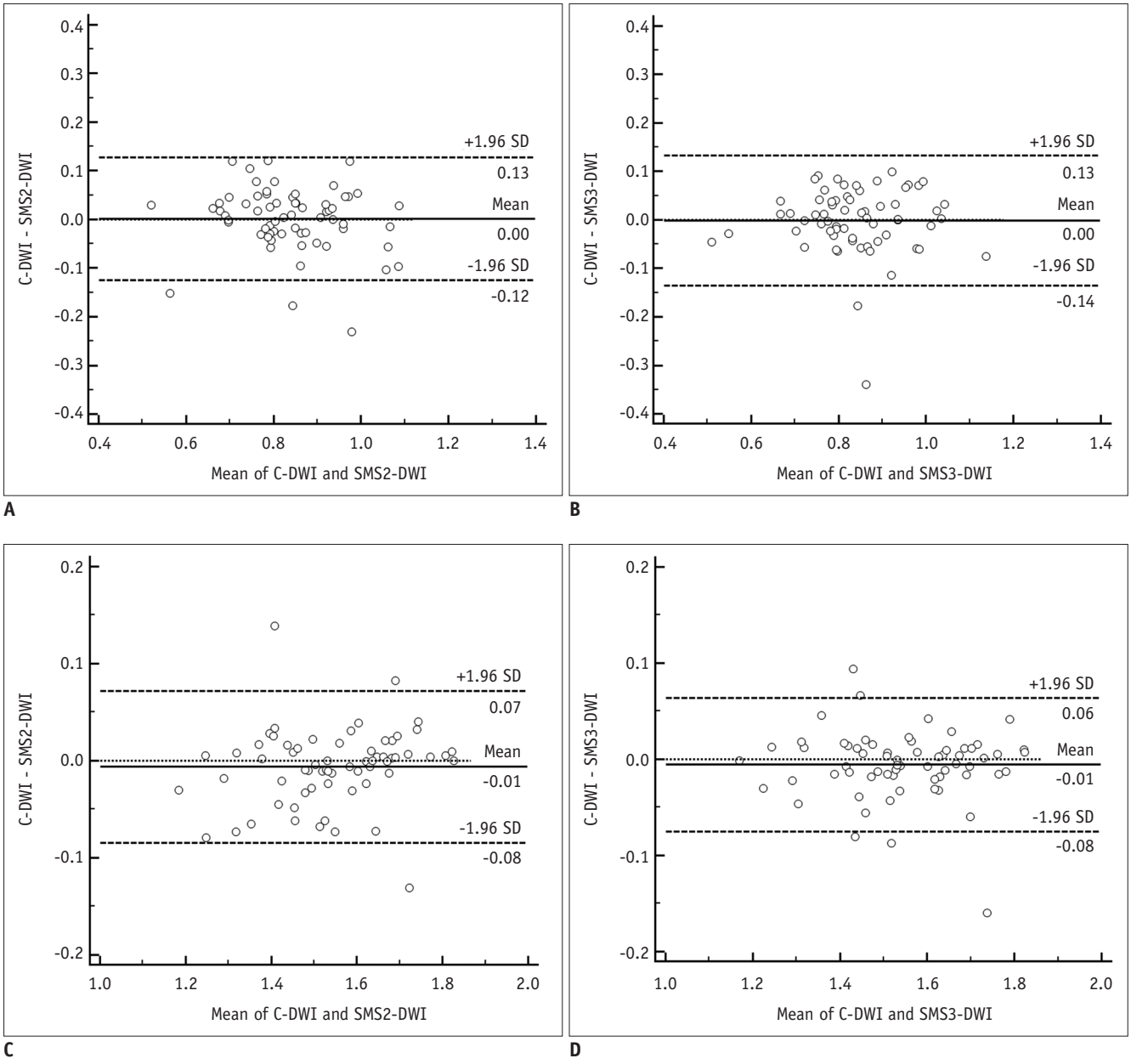

Fig. 4. Bland-Altman plots comparing ADC values of rectal cancer between C-DWI and SMS2-DWI (A) and between C-DWI and SMS3-DWI (B) and comparing ADC values of normal rectal wall between C-DWI and SMS2-DWI (C) and C-DWI and SMS3-DWI (D).
ADC values are given in x 10^{-3} mm^2/s. Solid line indicates mean absolute difference between two sequences, and dashed lines indicate 95% confidence interval of mean difference. SD = standard deviation

of MR scanners with different field strengths was not performed. The effect of field strength on the unaliasing of simultaneously obtained slices or susceptibility artifacts of SMS-DWI could thus not be evaluated.

In conclusion, SMS-DWI using an acceleration factor of 2 is feasible for rectal MRI, with a substantial reduction in acquisition time while maintaining a similar diagnostic image quality compared to C-DWI. In addition, ADC values were similar between SMS-DWI and C-DWI, which is a prerequisite for diagnostic evaluation.

Conflicts of Interest

The authors have no potential conflicts of interest to disclose.

ORCID iDs

Nieun Seo
https://orcid.org/0000-0001-8745-6454

 https://doi.org/10.3348/kjr.2019.0406

Jae Hyon Park
https://orcid.org/0000-0002-7626-194X
Joon Seok Lim
https://orcid.org/0000-0002-0334-5042
Jongmoon Hahm
https://orcid.org/0000-0001-5264-4367
Myeong-Jin Kim
https://orcid.org/0000-0001-7949-5402

REFERENCES

1. Jemal A, Siegel R, Xu J, Ward E. Cancer statistics, 2010. *CA Cancer J Clin* 2010;60:277-300
2. Kaur H, Choi H, You YN, Rauch GM, Jensen CT, Hou P, et al. MR imaging for preoperative evaluation of primary rectal cancer: practical considerations. *Radiographics* 2012;32:389-409
3. KSAR Study Group for Rectal Cancer. Essential items for structured reporting of rectal cancer MRI: 2016 consensus recommendation from the Korean Society of Abdominal Radiology. *Korean J Radiol* 2017;18:132-151
4. Liu L, Liu Y, Xu L, Li Z, Lv H, Dong N, et al. Application of texture analysis based on apparent diffusion coefficient maps in discriminating different stages of rectal cancer. *J Magn Reson Imaging* 2017;45:1798-1808
5. Lu ZH, Hu CH, Qian WX, Cao WH. Preoperative diffusion-weighted imaging value of rectal cancer: preoperative T staging and correlations with histological T stage. *Clin Imaging* 2016;40:563-568
6. Choi MH, Oh SN, Rha SE, Choi JI, Lee SH, Jang HS, et al. Diffusion-weighted imaging: apparent diffusion coefficient histogram analysis for detecting pathologic complete response to chemoradiotherapy in locally advanced rectal cancer. *J Magn Reson Imaging* 2016;44:212-220
7. Curvo-Semedo L, Lambregts DM, Maas M, Thywissen T, Mehsen RT, Lammering G, et al. Rectal cancer: assessment of complete response to preoperative combined radiation therapy with chemotherapy--conventional MR volumetry versus diffusion-weighted MR imaging. *Radiology* 2011;260:734-743
8. Park MJ, Kim SH, Lee SJ, Jang KM, Rhim H. Locally advanced rectal cancer: added value of diffusion-weighted MR imaging for predicting tumor clearance of the mesorectal fascia after neoadjuvant chemotherapy and radiation therapy. *Radiology* 2011;260:771-780
9. Beets-Tan RGH, Lambregts DMJ, Maas M, Bipat S, Barbaro B, Curvo-Semedo L, et al. Magnetic resonance imaging for clinical management of rectal cancer: updated recommendations from the 2016 European Society of Gastrointestinal and Abdominal Radiology (ESGAR) consensus meeting. *Eur Radiol* 2018;28:1465-1475
10. Feinberg DA, Moeller S, Smith SM, Auerbach E, Ramanna S, Gunther M, et al. Multiplexed echo planar imaging for sub-second whole brain FMRI and fast diffusion imaging. *PLoS One* 2010;5:e15710
11. Xu J, Moeller S, Auerbach EJ, Strupp J, Smith SM, Feinberg DA, et al. Evaluation of slice accelerations using multiband echo planar imaging at 3 T. *Neuroimage* 2013;83:991-1001
12. Moeller S, Yacoub E, Olman CA, Auerbach E, Strupp J, Harel N, et al. Multiband multislice GE-EPI at 7 tesla, with 16-fold acceleration using partial parallel imaging with application to high spatial and temporal whole-brain fMRI. *Magn Reson Med* 2010;63:1144-1153
13. Van Essen DC, Ugurbil K, Auerbach E, Barch D, Behrens TE, Bucholz R, et al.; WU-Minn HCP Consortium. The Human Connectome Project: a data acquisition perspective. *Neuroimage* 2012;62:2222-2231
14. Taron J, Martirosian P, Erb M, Kuestner T, Schwenzer NF, Schmidt H, et al. Simultaneous multislice diffusion-weighted MRI of the liver: analysis of different breathing schemes in comparison to standard sequences. *J Magn Reson Imaging* 2016;44:865-879
15. Kenkel D, Barth BK, Piccirelli M, Filli L, Finkenstädt T, Reiner CS, et al. Simultaneous multislice diffusion-weighted imaging of the kidney: a systematic analysis of image quality. *Invest Radiol* 2017;52:163-169
16. Weiss J, Martirosian P, Taron J, Othman AE, Kuestner T, Erb M, et al. Feasibility of accelerated simultaneous multislice diffusion-weighted MRI of the prostate. *J Magn Reson Imaging* 2017;46:1507-1515
17. Filli L, Piccirelli M, Kenkel D, Guggenberger R, Andreisek G, Beck T, et al. Simultaneous multislice echo planar imaging with blipped controlled aliasing in parallel imaging results in higher acceleration: a promising technique for accelerated diffusion tensor imaging of skeletal muscle. *Invest Radiol* 2015;50:456-463
18. Lau AZ, Tunnicliffe EM, Frost R, Koopmans PJ, Tyler DJ, Robson MD. Accelerated human cardiac diffusion tensor imaging using simultaneous multislice imaging. *Magn Reson Med* 2015;73:995-1004
19. Ciritsis A, Rossi C, Marcon M, Van VDP, Boss A. Accelerated diffusion-weighted imaging for lymph node assessment in the pelvis applying simultaneous multislice acquisition: a healthy volunteer study. *Medicine (Baltimore)* 2018;97:e11745
20. Dyde R, Chapman AH, Gale R, Mackintosh A, Tolan DJ. Precautions to be taken by radiologists and radiographers when prescribing hyoscine-N-butylbromide. *Clin Radiol* 2008;63:739-743
21. Taron J, Martirosian P, Kuestner T, Schwenzer NF, Othman A, Weiß J, et al. Scan time reduction in diffusion-weighted imaging of the pancreas using a simultaneous multislice technique with different acceleration factors: how fast can we go? *Eur Radiol* 2018;28:1504-1511
22. Barth M, Breuer F, Koopmans PJ, Norris DG, Poser BA. Simultaneous multislice (SMS) imaging techniques. *Magn Reson Med* 2016;75:63-81
23. Gagoski BA, Bilgic B, Eichner C, Bhat H, Grant PE, Wald LL,

https://doi.org/10.3348/kjr.2019.0406

et al. RARE/turbo spin echo imaging with simultaneous multislice wave-CAIPI. *Magn Reson Med* 2015;73:929-938
24. Obele CC, Glielmi C, Ream J, Doshi A, Campbell N, Zhang HC, et al. Simultaneous multislice accelerated free-breathing diffusion-weighted imaging of the liver at 3T. *Abdom Imaging* 2015;40:2323-2330
25. Boss A, Barth B, Filli L, Kenkel D, Wurnig MC, Piccirelli M, et al. Simultaneous multi-slice echo planar diffusion weighted imaging of the liver and the pancreas: optimization of signal-to-noise ratio and acquisition time and application to intravoxel incoherent motion analysis. *Eur J Radiol* 2016;85:1948-1955
26. Taron J, Weiß J, Martirosian P, Seith F, Stemmer A, Bamberg F, et al. Clinical robustness of accelerated and optimized abdominal diffusion-weighted imaging. *Invest Radiol* 2017;52:590-595
27. Peng Y, Li Z, Tang H, Wang Y, Hu X, Shen Y, et al. Comparison of reduced field-of-view diffusion-weighted imaging (DWI) and conventional DWI techniques in the assessment of rectal carcinoma at 3.0T: image quality and histological T staging. *J Magn Reson Imaging* 2018;47:967-975
28. Akashi M, Nakahusa Y, Yakabe T, Egashira Y, Koga Y, Sumi K, et al. Assessment of aggressiveness of rectal cancer using 3-T MRI: correlation between the apparent diffusion coefficient as a potential imaging biomarker and histologic prognostic factors. *Acta Radiol* 2014;55:524-531
29. Dietrich O, Raya JG, Reeder SB, Reiser MF, Schoenberg SO. Measurement of signal-to-noise ratios in MR images: influence of multichannel coils, parallel imaging, and reconstruction filters. *J Magn Reson Imaging* 2007;26:375-385

 https://doi.org/10.3348/kjr.2019.0406